RSC Advances

This is an *Accepted Manuscript*, which has been through the Royal Society of Chemistry peer review process and has been accepted for publication.

Accepted Manuscripts are published online shortly after acceptance, before technical editing, formatting and proof reading. Using this free service, authors can make their results available to the community, in citable form, before we publish the edited article. This *Accepted Manuscript* will be replaced by the edited, formatted and paginated article as soon as this is available.

You can find more information about *Accepted Manuscripts* in the Information for Authors.

Please note that technical editing may introduce minor changes to the text and/or graphics, which may alter content. The journal's standard Terms & Conditions and the Ethical guidelines still apply. In no event shall the Royal Society of Chemistry be held responsible for any errors or omissions in this *Accepted Manuscript* or any consequences arising from the use of any information it contains.

ROYAL SOCIETY OF CHEMISTRY

www.rsc.org/advances

RSC Advances

ARTICLE

Tethering silver ion on Amino-functionalized mesoporous silica for enhanced and sustained antibacterial properties

Received 00th January 20xx,
Accepted 00th January 20xx

DOI: 10.1039/x0xx00000x

www.rsc.org/

Chengwei Wang,[a, b] Hua Hong,[a, c]*, Zhaofen Lin,[c] Yuan Yuan,[a, c]* Changsheng Liu,[a, b, c] * Xiaoyu Ma,[a, b] Xiaoyan Cao,[a, b]

Silver ions were tethered onto amino-functionalized Ca-doped mesoporous silica (CaMSS) via complexing action of Ag^+-NH_2 for the antibacterial property. Flourier-transform infrared (FTIR), transmission electron microscopy (TEM), and energy dispersive spectroscopy (EDS) indicated the successful tethering of silver ions onto CaMSS and the complexing action of amino groups enabled the silver ion to be more stable than that adsorbed without amino group. Minimum inhibitory concentration (MIC) and growth-curve experiments were utilized to test and compare the time- and concentration-dependent antibacterial capability of silver ions tethered- and adsorbed-CaMSS with Escherichia coli (E. coil) as bacteria model. The results showed that at the same silver ion loading, surface-tethered Ag-CaMSS possessed longer-term, and more efficiency (2.5 times lower MIC) antibacterial activity during the whole test period compared to the silver ions-adsorbed CaMSS. But with the increasing of the amount of amino groups, the antibacterial activity was not obviously changed. Further studies demonstrated that the excellent and sustained antibacterial efficiency of silver-tethered CaMSS should be attributed to the stable amino group-based complexing action with Ag, strong interaction of positively-charged CaMSS surface to negatively-charged bacteria, and the strong inhibition effect of Ag^+ and agglomerates of silver chloride localized onto theCaMSS surface. All taken, this amino group-based tethering method is an effective strategy to load Ag ion for sustained and high efficient antibacterial activity. This developed Ag-CaMSS is a promising surgical implantation with excellent antibacterial activity.

Introduction

Current medical advancement has been characterized by the broadest application of medical devices in all fields, especially the indwelling implants in surgery[1]. Unfortunatedly, implant-associated infection often remains a significant clinical challenge [2, 3]. In particular, the overall number of such infections has been continuously increasing with the growing demands for surgical implantation as a result of population aging and mounting participation in recreational activities[4].Therefore, it is highly desirable to develop implanted biomaterials with excellent antibacterial properties.

Nowadays, mesoporous silica (MSS) have attracted extensive attention due to their unique physicochemical (including ordered porous structure, large internal surface area and volume, size controllability, and easy functionalization), facile synthetic methods, and their broad range of applications[5-8]. In particular, owing to the excellent biocompatibility and the functional versatility, MSS have been successfully employed as controlled release systems for drugs[9, 10], antimicrobial carriers[11, 12] (encapsulated antibacterial agents) and bone regeneration materials[13, 14]. But, just as other biomaterials, MSSs also present an increased risk for biofilm-associated infections. To overcome this problem, currently, a serial of antibacterial agents, like antibiotics, polypeptides, inorganic nanoparticles and metal ions[11, 12, 15, 16] have been developed for protecting MSS-related bio-application against bacteria fouling. Although antibiotics exhibit great effectiveness, fast development of resistances and poor surface protecting largely hampered its application[17]. As for polypeptides, they are easy to lose activation, leading to short effective period[11]. In comparison, silver nanoparticles (Ag NPs) have been proven to possess excellent antimicrobial activity against a broad spectrum of pathogens and Ag NPs encapsulated in nano-sized mesoporous silica (Ag@MSS) represent one of the most popular antibacterial materials[12]. A large number of studies have indicated that the bactericidal properties of Ag NPs depend primarily on the release of silver ions[18, 19], which can interact with the cell

[a] Key Laboratory for Ultrafine Materials of Ministry of Education, East China University of Science and Technology, Shanghai 200237, PR China.
[b] Engineering Research Center for Biomedical Materials of Ministry of Education, East China University of Science and Technology, Shanghai 200237, PR China.
[c] The Second Military Medical University, Shanghai 200433, PR China.

Email:hhong@ecust.edu.cn, yyuan@ecust.edu.cn, liucs@ecust.edu.cn

RSC Advances Accepted Manuscript

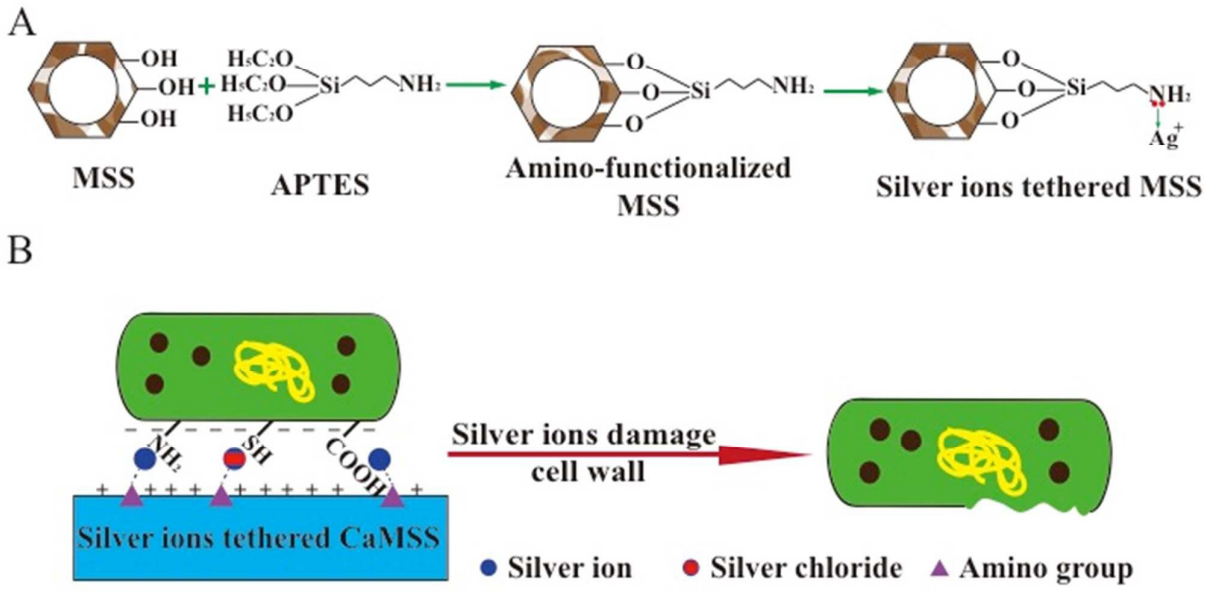

Fig 1.A, Schematic procedure for the surface modification of MSS and the subsequent immobilization of silver ions on the surface modified MSS. B，Schematic drawing of silver ions deactivate biological group and destroy the bacterial wall.

envelope protein and enzymes of bacteria containing imidazole, amino, carboxyl, and thiol groups, and eventually cause the death of bacteria[20-22]. Nevertheless, the Ag NPs loaded in Ag@MSS could not directly contact with microorganisms and be fully utilized, especially in early stage of release[18, 19]. To overcome this problem, silver ions were introduced into MSS by ion exchange[16]. Such composites can effectively enhance the antibacterial activity，but the release of silver ions was fast, leading to a rapid decrease and short-term of antibacterial activity. Therefore, it is of great importance to develop a silver ions-loaded MSS with high and long-term antibacterial properties.

Herein, we endeavored to develop an effective route to tether silver ion onto the surface of MSS via the amino-based complexing action. The amino group was first grafted onto the surface of MSS by the addition of (3-Aminopropyl)-trimethoxysilane (APTES), and then the silver ion was tethered with the aminopropyl groups (Fig 1A). On one hand, the amino groups can turn the negative surface charge of MSS to positive[9] and thus increase the interactionof MSS particle with the negatively charged bacterial surface. On the other hand, amino-based complexing action can maintain a localized and concentrated silver ion, enabling the surface-tethered silver ion or silver chloride agglomerate to directly deactivate biological groups by electrostatic interactions between amino-functionalized MSS and bacterial, thus to destroy the cell wall, leading to the death of bacteria (Fig 1B).The effects of theamount of amino group on mesoporous silica structure and antibacterial properties were studied. For comparison, a silver ion-adsorbed MSS was also prepared. In order to investigate the long-time antibacterial activity and antibacterial efficiency, the minimum inhibitory concentration (MIC) and growth-curve experiments were carried out to characterize the antibacterial activity of silver and MSS hybrids as well as silver and amino functionalized MSS hybrids.

Experimental

Materials

Commercially available chemicals were used as received. Pluronictriblock copolymer P123 (EO20PO30EO20) and (3-Aminopropyl)-trimethoxysilane (APTES) were purchased from Sigma Aldrich Chemicals and adopted as pore structure-directing agents (SDA) and coupling agent (CA). Tetraethylorthosilicate (TEOS), $Ca(NO_3)_2 \cdot 4H_2O$ were purchased from Shanghai Sinopharm and used for materials preparation. Deionized water was used throughout this work and all other chemicals used were of analytical grade.

Synthesis of mesoporous silica

Ordered mesoporous silica was synthesized according to a previously reported procedure[23]. Briefly, a typical silica sol was prepared with a molar ratio of TEOS: H_2O: HCL: P123 = 0.082: 13.33: 0.48: 0.001. Meanwhile, $Ca(NO_3)_2 \cdot 4H_2O$ was added into the solution as calcium oxide precursors. The mixture was stirred magnetically at 35 ^{o}C for 24 h and a certain amount of ammonia was poured into the reaction system at the end of reaction. After continuous stirring for 30 min, the products were collected by vacuum filtering, washed repeatedly by

RSC Advances Accepted Manuscript

ethanol and water, and dried at 60 °C. The surfactant was removed by calcination in air at 600 °C for 6 h with the ramping rate of 1 °C min^{-1}. The as-synthesized CaMSS were stored in a desiccator at room temperature before usage.

Amino-functionalized and silver loaded CaMSS

Amino group was functionalized onto CaMSS by treatment with APTES in absolute ethanol to avoid undesirable side reactions between CA and water[11, 24]. Briefly, CaMSS was first dispersed in absolute ethanol, followed by the addition of a given mass of APTES, stirred for 4 h at 60 °C, rotary evaporated the solvent and dried at 60 °C. The samples were named as CaMSS-0.5N and CaMSS-1N, respectively, where the number 0.5 and 1 represented the volume of APTES added to per gram CaMSS in the process of amino functionalization. At the same time, the unfunctionalizedCaMSS was marked as CaMSS-0N.

The silver was loaded in the following steps. In detail, 2 g of amino-functionalized powder was dispersed in absolute ethanol and a certain amount of silver nitrate was added and stirred for 30 min. The products, marked as CaMSS-0.5N-Ag and CaMSS-1N-Ag respectively, were collected by rotary evaporating the solvent and drying at 60°C. In comparison, a silver ion-adsorbed CaMSS, named as CaMSS-0N-Ag, was also prepared and the silver-loaded procedure was the same to the above steps of sliver loading in the functionalized CaMSS.

Characterization

The ordered mesoporous structure of samples was confirmed by small-angle X-ray diffraction (SAXRD, Rigaku D/max 2550VB/PC, Japan) and transmission electron microscopy (TEM, JEM-1400, JEOL, Japan). Surface analysis of the MSS was performed by N_2 adsorption/desorption measurement on a Micromeritics ASAP2010 sorptometer (Micromeritics, USA). Prior to detection, the samples were degassed at 100 °C under vacuum for 4 h. The specific surface area was determined by the Bruaauer Emmett-Teller (BET) method and the pore parameters (pore volume and pore diameter) were obtained from the adsorption branch on the basis of Barrett-Joyner-Halenda (BJH) model.

The flourier-transform infrared (FTIR) spectra were obtained using a Perkine Elmer System2000 spectrometer (Nicolet Magma-550 series II, Midac, USA) from KBr pellets at wavelengths ranging from 4000 to 400 cm^{-1}at a resolution of 1 $cm^{-1}$with an average of 64 scans. The elements of the samples were confirmed by energy dispersive spectroscopy (EDS, attached to the scanning electron microscope (SEM，JSM-6360LV，JEOL，Japan).

Electrophoretic mobility measurement was performed to measure the surface charge (z-potential) of the MSS particles. The electrophoretic mobility assay was adapted from Dai. C *et al* and Jessica M. Rosenholm*et al*[16, 25]. The zeta-potential was measured as a function of pH by titrating with 0.5 M HCl and NaOH at 25°C. The samples were suspended in 2.5 mmol L^{-1} of $CaCl_2$ aqueous (1 mg mL^{-1}) and dispersed by sonication. Reverse titrations were performed to ensure chemical stability of the introduced surface function during the measurements.

Growth-curve experiments

Growth-curve experiments adapted from Monty Liong*et al*[12] were used to evaluate the antimicrobial efficacy of various samples containing different amounts of amino group. Briefly, E. Coli (ATCC 25922) was cultured in LB medium (Bacto-Tryptone 10 g L^{-1}, Bacto-yeast extract 5 g L^{-1}, NaCl 10 g L^{-1}, pH 7.2~7.4) at 37 °C on a shaker bed at 80 rpm for 4-6 h. Then the concentration of bacteria, corresponding to an optical density of 0.1 at 600 nm for 1×10^8 CFU mL^{-1} diluted with LB medium, was measured by UV-vis spectroscopy. For growth-curve experiments, various concentrations of the synthesized CaMSS, CaMSS-0N-Ag, CaMSS-0.5N-Ag and CaMSS-1N-Ag were then added to the culture plate and the turbidity measurements were taken over a time course.

Minimum Inhibitory Concentration (MIC)

The MIC assay was adapted from Wang hao*et al*[11]. The E. coil was cultured by the same procedure as described above. The bacterial suspension (20 μL of 1×10^6 CFU mL^{-1}) was added into LB medium (180 μL) for each well. Then samples were separately added into 96-well plates and shaken at 37 °C on a shaker bed at 80 rpm for 24 h. The bacterial viability was determined at OD 600 nm using a multifunctional micro plate reader. Each concentration was prepared and measured in triplicate, and all experiments were repeated at least twice in parallel.

Morphological change of E. coil

To visualize the morphology of the E. coil treated with the CaMSS-0N-Ag and CaMSS-0.5N-Ag, we first prepared the CaMSS-0N-Ag and CaMSS-0.5N-Ag disc and then sterilized them under UV radiation for 2 h at room temperature. After sterilization, the sample discs were placed on 24-well plates, followed by the addition of 2 mL of 1×10^8 CUF mL^{-1} E. coil and cultured at 37 °C.

At each incubation interval, the samples were rinsed with PBS twice and fixed with 2.5% glutaraldehyde. Before SEM examination, the samples were dehydrated in gradient ethanol solutions (30, 50, 70, 80, 90, 95 and 100 v/v %) for 10 min sequentially, then immersed in tert-butyl alcohol and dried. The samples with cells were coated with gold before SEM examination.During the examination, the working voltage was performed at 15 kV.

***In vitro* cytotoxicity assays**

RSC Advances Accepted Manuscript

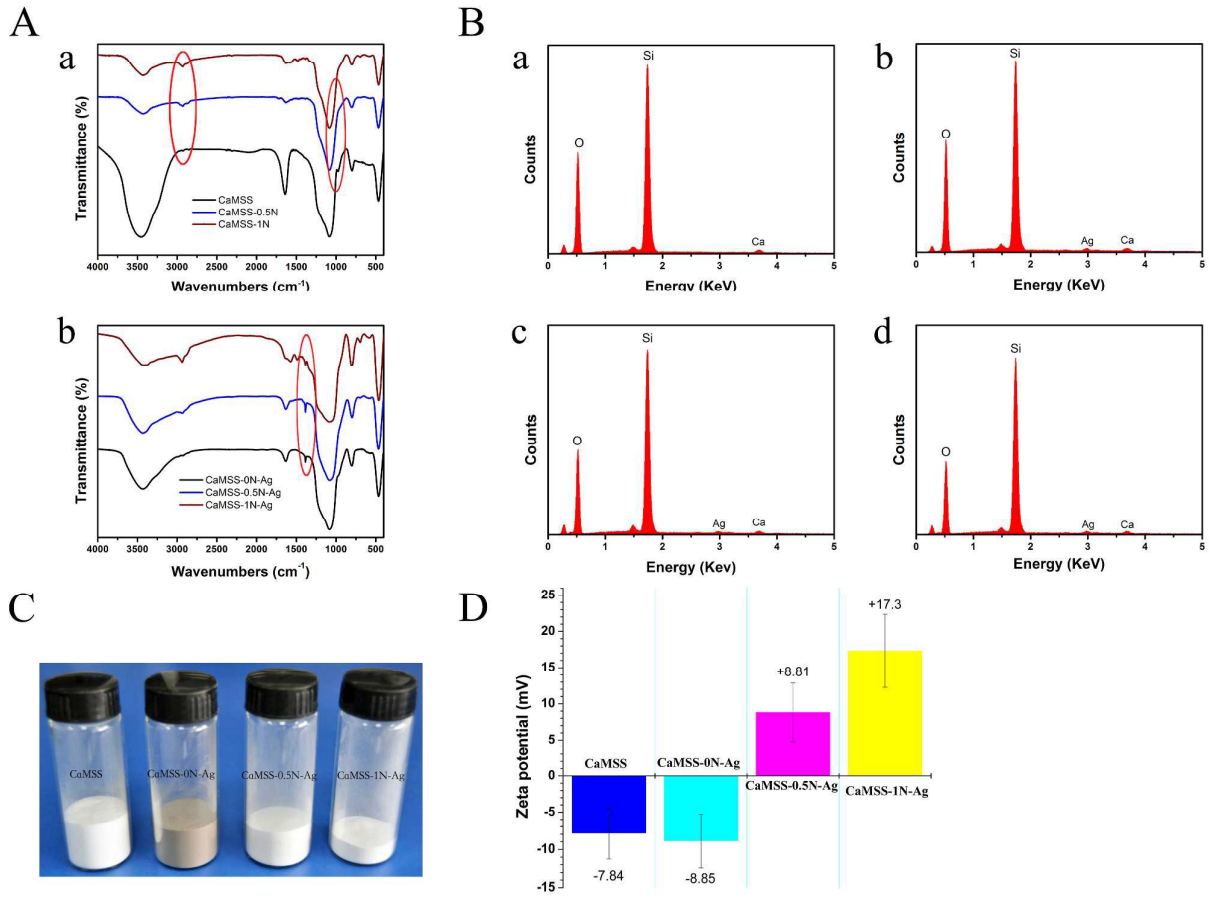

Fig 2. A, FTIR spectra of samples: a, CaMSS before and after amino functionalized; b, silver loaded onto amino-functionalized CaMSS. B, EDS characterize of samples: a, CaMSS; b, CaMSS-0N-Ag; c, CaMSS-0.5N-Ag; d, CaMSS-1N-Ag. C, Photographes of samples. D, Zeta potential of the samples at pH 7.4.

The cytotoxicity of the prepared samples was investigated by MTT assays using mouse myoblast cells line (ACTT, C2C12). The samples in media without cells were tested and found that they do not interfere with the MTT assay. Briefly, C2C12 cells were cultured in Dulbecco's Modified Eagle's Medium (DMEM) with 0.11 g L^{-1} L-glutamine, 2.2 g L^{-1} sodium bicarbonate, 10% fetal bovine serum and 2% antibiotics (200 mg mL^{-1} penicillin and 200 mg mL^{-1} streptomycin) for 8 days. Medium was changed twice a week. The cells from passages 5 through 15 were seeded into 96 well plates at a density of 5000 cells per well and then were exposed to various amounts of CaMSS, CaMSS-0N-Ag and CaMSS-1N-Ag, in the range of 0.1-0.25 mg mL^{-1}. After incubation in a fully humidified atmosphere of 5% CO_2 at 37 ^{o}C for 24 h, the cell viabilities were assessed by MTT assays. The results were reported by means of at least three wells and presented as viability of cells compared with negative control (TCPS).

Results and discussion

Amino- and silver-functionalized CaMSS

The successful functionalizationof amino group CaMSS and further tethering of silver ion- CaMSS were confirmed by FTIR spectra. As shown in Fig 2A (a), CaMSS displayed a typical FTIR spectrum of mesoporous silica. The peak at 3450 cm^{-1} was assigned to stretching vibration of hydrogen bonded silanol group υ(≡Si-OH) and υ(-OH) of physisorbed water molecule. The peak at 1640 cm^{-1} was attributed to O-H bending vibration mode of physisorbed water molecule. The peaks of Si–O–Si asymmetric stretching vibration, symmetric stretching vibration and bending vibration were observed at 1083 cm^{-1}, 800 cm^{-1} and 465 cm^{-1}. The peak at 972 $cm^{-1}$was attributed to υ(≡ Si-OH) of free silanol group[5]. After amino-functionalization, the spectrum of the CaMSS displayed almost

RSC Advances Accepted Manuscript

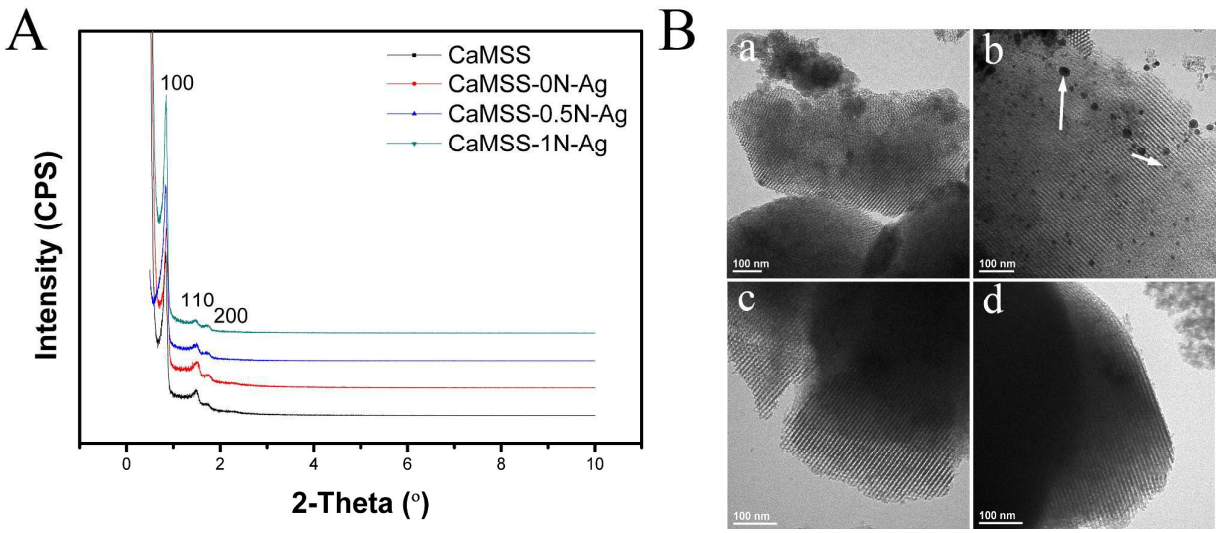

the same characteristic bands of CaMSS except for a slight decrease of the intensity of the free silanol group at 972 $cm^{-1}$and appearance of sharp bands at 2930 cm^{-1}corresponding to υ(-CH_2-) stretching spectra[10]. The intensity of the stretching vibration of the methylene increased with the increase of the amount of APTES. However, after silver nitrate addition, the absorption band at around 1385 cm^{-1} emerged in the sample, which could be assigned to N=O stretching of $AgNO_3$ on silver-loaded CaMSS both with and without amino-functionalization (Fig 2A(b)).

Fig 3. A, XRD patterns of samples. B, TEM images of samples: a，CaMSS; b, CaMSS-0N-Ag; c, CaMSS-0.5N-Ag; d, CaMSS-1N-Ag.

EDS assay confirmed the successful tetheringof silver ions in the CaMSS samples (Fig 2B). The content of the silver was almost the same, about 1.4% (W/W). In the experiment, the molar ratio of amino groups and silver ions was 10:1 for CaMSS-0.5N-Ag. Therefore, the silver ions, whether in the sample of CaMSS-1N-Ag or CaMSS-0.5N-Ag, were completely complexed with amino groups. So, the amount of silver in the samples was kept at the same level in CaMSS-1N-Ag or CaMSS-0.5N-Ag.

From Fig 2C, it can be seen that the silver-loaded CaMSSvia amine tethering exhibited different color with various silver-adsorbed CaMSS. Specifically, the color of CaMSS-0N was changed to gray, but the CaMSS-0.5N and CaMSS-1N showed the same white color as CaMSS. These results indicated that silver existedin different state in the samples with amino functionalized and unfunctionalizedCaMSS. The appearance of nanoparticles in CaMSS-0N-Ag in TEM image (Fig 3B (b), the white arrow pointed) also confirmed this result. The color change of CaMSS-0N-Ag and Agnanoparticle deposit may be

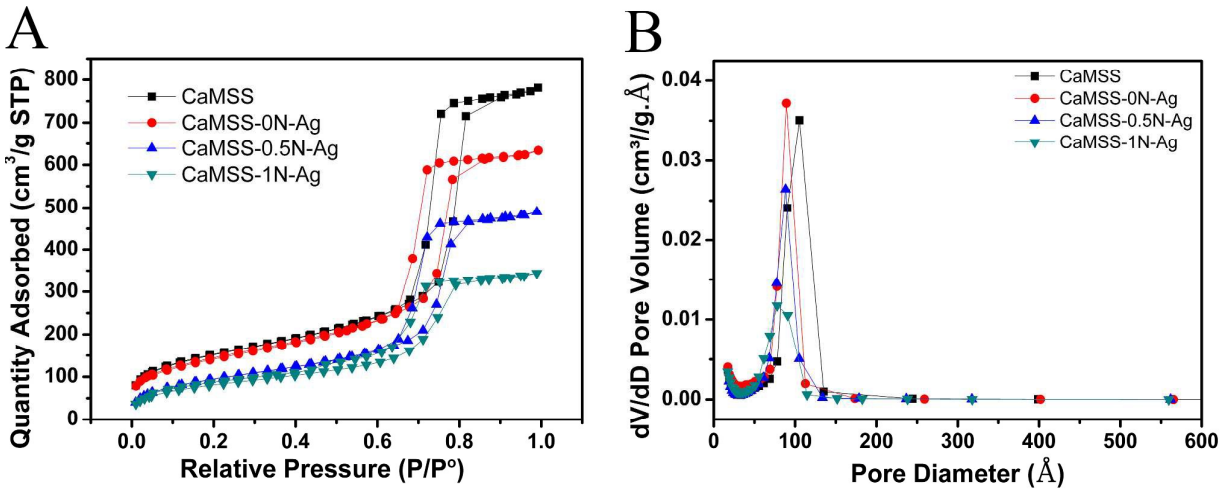

RSC Advances Accepted Manuscript

Fig 4. A, N_2 adsorption/desorption isotherms of samples.B, the corresponding pore-size distribution of samples.

Table 1. Textural parameters of Samples: Specific surface area (S_{BET}), mesopore volume (V_p) and pore size (D_p).

	CaMSS	CaMSS-0N-Ag	CaMSS-0.5N-Ag	CaMSS-1N-Ag
S_{BET} (m^2/g)	534.12	512.15	347.57	292.47
V_p (cm^3/g)	1.19	0.96	0.74	0.52
D_p (nm)	9.18	7.71	8.16	7.02

caused by the degeneration of silver nitrate, andCaMSS-0.5N-Ag and CaMSS-1N-Ag can serve as stabilized carriers.

As anticipated, the surface charge of silver-tethered CaMSS was detected by zeta potential measurements in 2.5 mmol L^{-1} of $CaCl_2$ aqueous at pH 7.4 (Fig 2D). It can be observed that the zeta potential of the CaMSS was -7.84 mV, and the zeta potential ofCaMSS-0N-Ag was decreased to -8.85 mV. But when silver ions was tethered onto the surface of CaMSS, the surface charge turned to positive +8.81 mV and +17.3 mV for the sample of CaMSS-0.5N-Ag and CaMSS-1N-Ag, respectively.

Microstructure of the CaMSS and silver-tethered CaMSS

To investigate the influence of the silver tethering and amount of amino groups on the mesoporous silica structure, XRD, TEM and N_2 adsorption and desorption characterization were conducted. XRD patterns (Fig 3A) of CaMSS before and after functionalization showed three diffraction peaks, which can be indexed to the 100,110, 200 Bragg reflection peaks for a highly ordered hexagonal mesostructure (space group of p6mm)[26]. TEM (Fig 3B) confirmed that the ordered pore structure assembly remained very well even afteramino-functionalization with different volume of APTES and silver loading[10]. Shown in Fig 3B (b), a lot of nanoparticles were deposited on the surface or in the pores, which might be caused by the degeneration of silver nitrate, consistent with the result of the color change of samples.

Fig. 4 showed the N_2 adsorption/desorption isotherms and pore size distributions of CaMSS before and after functionalization. All samples revealed typical IV with H1-type hysteresis loops, indicating rod-like pores in these mesoporous nanoparticles. The sharp capillary condensations in the range of relative pressure of 0.6-0.8 suggested a uniform pore sizedistribution[10]. The BET surface areas (S_{BET}) of the CaMSSwas 534.12 m^2 g^{-1} and the pore diameters (D_p) was 9.18 nm, respectively, while the S_{BET} and D_p of CaMSS-0N-Ag was decreased to 512.15 m^2 g^{-1} and 7.71 nm (Table 1). However, when the amino groups were grafted onto the surface of the CaMSS, the textural properties, S_{BET} and D_P, became 347.57 m^2 g^{-1}, 8.16 nm and 292.47m^2 g^{-1}, 7.02nm (Table 1) for the sample of CaMSS-0.5N-Agand CaMSS-1N-Ag, respectively. It can be concluded that the there was a decrease in diameter of the sample with amino functionalization and silver loading. From the above results, it could be proven that the introduction of amino groups and tetheringof silver did not lead to changes of the order degree of CaMSS. However, with the increase of amino added to per gram CaMSS, confirmed by N_2 adsorption/desorption, the textural properties, S_{BET}, V_P, D_P, were decreased to some extent.

Growth-curve experiment

It was known to all that silver ion possesses great antibacterial property. Herein, we investigated and compared the time- and concentration-dependent antibacterial ability of silver-loaded CaMSS via various processes. Fig 5A illustrated the images of the bacteria co-cultured with various concentrations of CaMSS, CaMSS-0N-Ag, CaMSS-0.5N-Ag and CaMSS-1N-Ag after 8 h's treatment. It can be inferred that CaMSS had no influence on the growth of E. coil, CaMSS-0N-Ag exerted obvious effect on the bacteria growth at higher concentration of 200 μg mL^{-1}, while CaMSS-0.5N-Ag and CaMSS-1N-Ag possessed significant inhibition on the growth of E. coil at all concentrations.

Based on the above results, the growth kinetics of bacteria in liquid media treated by silver-loaded CaMSS via various processes were further studied and compared at fixed concentration of 200 μg mL^{-1} (Fig 5B). The bacterial-growth was monitored by measuring the optical density at 600 nm (OD600) based on the turbidity of the cell suspension. For these experiments, bacteria were grown to the concentration of 1×10^8 CUF mL^{-1} (OD600 =0.1), diluted to 1×10^6 CUF mL^{-1}, and then mixed with CaMSS, CaMSS-0N-Ag, CaMSS-0.5N-Ag and CaMSS-1N-Ag. It can be seen the CaMSSdemonstrated a similar growth curve to that of the control group at all tested period, indicating it had no noticeable effect on E. coil growth. In the initial 6 h, CaMSS-0N-Ag, CaMSS-0.5N-Ag and CaMSS-1N-Ag were all able to slow the growth of E. coil. Nevertheless, after 20 h, the CaMSS-0N-Ag did not continue inhabiting the growth of E. coil. On the contrary, CaMSS-0.5N-Ag and CaMSS-1N-Ag could exert significant effect on the bacteria growth throughout the whole period.

E. coli was incubated in LB medium in a 96-well plate, and different amounts of samples were added to the E. coli and incubated for 24 h. Subsequently, the inhibition of proliferation of E. coli was utilized to estimate the antibacterial activity of CaMSS-0.5N-Ag and CaMSS-1N-Ag. In parallel, LB media, CaMSS and CaMSS-0N-Ag were set as controls for comparison (Fig5C). The MIC value of CaMSS-0.5N-Ag and CaMSS-1N-Ag toward E. coli was 100 μg mL^{-1}, which was 2.5

RSC Advances Accepted Manuscript

This journal is © The Royal Society of Chemistry 20xx

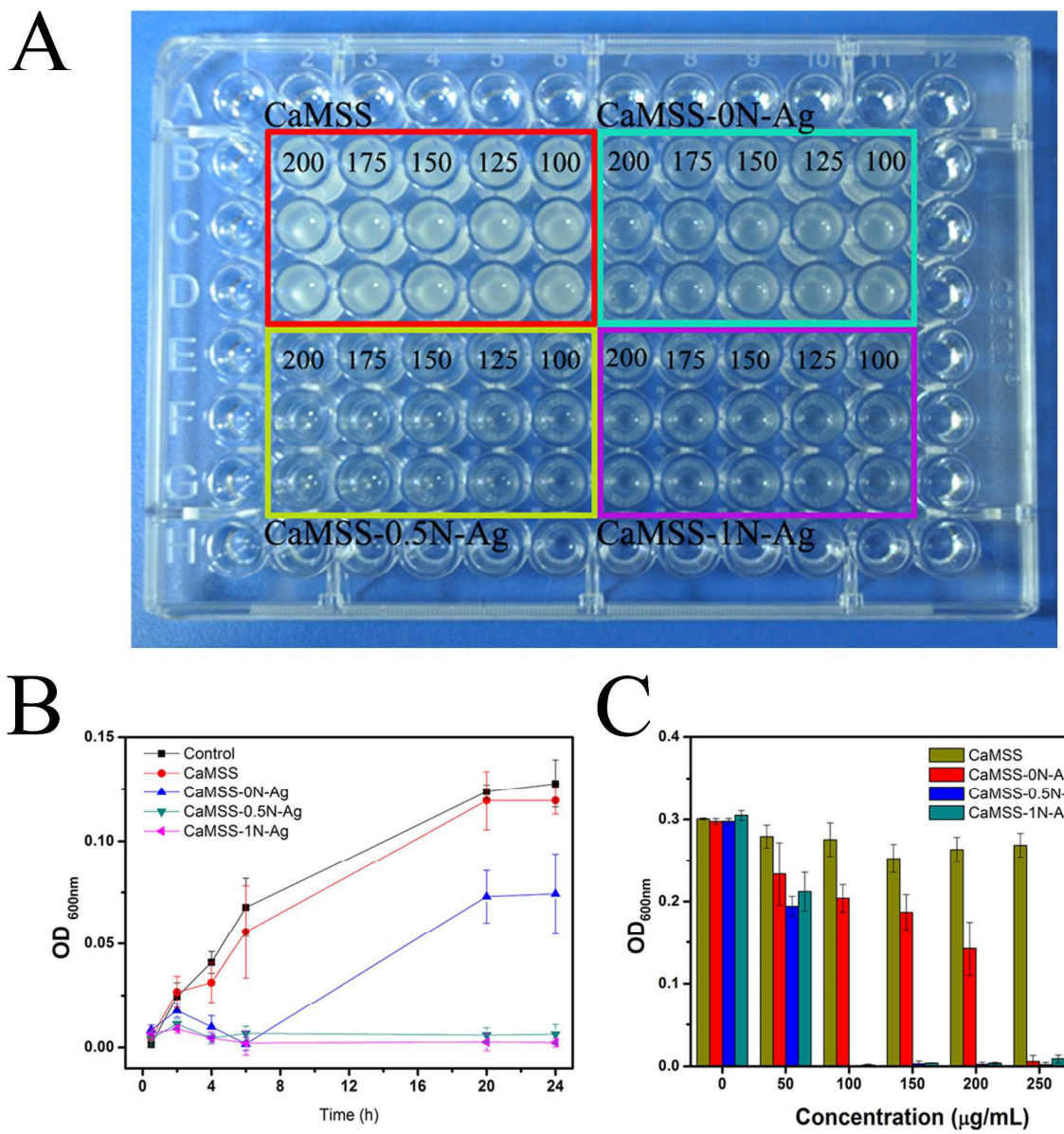

times lower than that of unfunctionalized CaMSS-0N-Ag withan MIC of 250 μg mL^{-1}. Obviously, the MICs results

Fig5. A, photograph of samples antibacterial activity on the different concentration after 8h treatment.B, Bacteria growth-curve in LB media.C, the antibacterial activity of samples toward E. coli was evaluated by OD600.

provided solid evidence that the CaMSS-0.5N-Ag and CaMSS-1N-Ag possessed higher antibacterial abilities than the CaMSS-0N-Ag in the same circumstances.

Morphology of E. coil on the CaMSS

SEM was utilized to examine the morphology and membrane integrity of E. coil after 30 min exposure to CaMSS and the results were displayed in Fig6. Compared with the CaMSS-0N-Ag (Fig 6A) at low magnification, it was noticed that spherical agglomerates comprising silver and chlorine, as determined by EDS (inserted in Fig6B (b), (c)), appeared on the surface of CaMSS-0.5N-Ag plate (Fig 6B). It, we think, should be attributable the precipitation of chloride ions in the culture medium and the surface-tethered silver ions of CaMSS-0.5N-Ag. Furthermore, under low magnification times, it can also be seen that the number of E. coil on the surface of CaMSS-0.5N-Ag was much more than that on CaMSS-0N-Ag (Fig 6A (a), B(a)). It can be inferred that the positively charged surface of amino functionalized CaMSSwas benefit tothe E. coil adsorption.

RSC Advances Accepted Manuscript

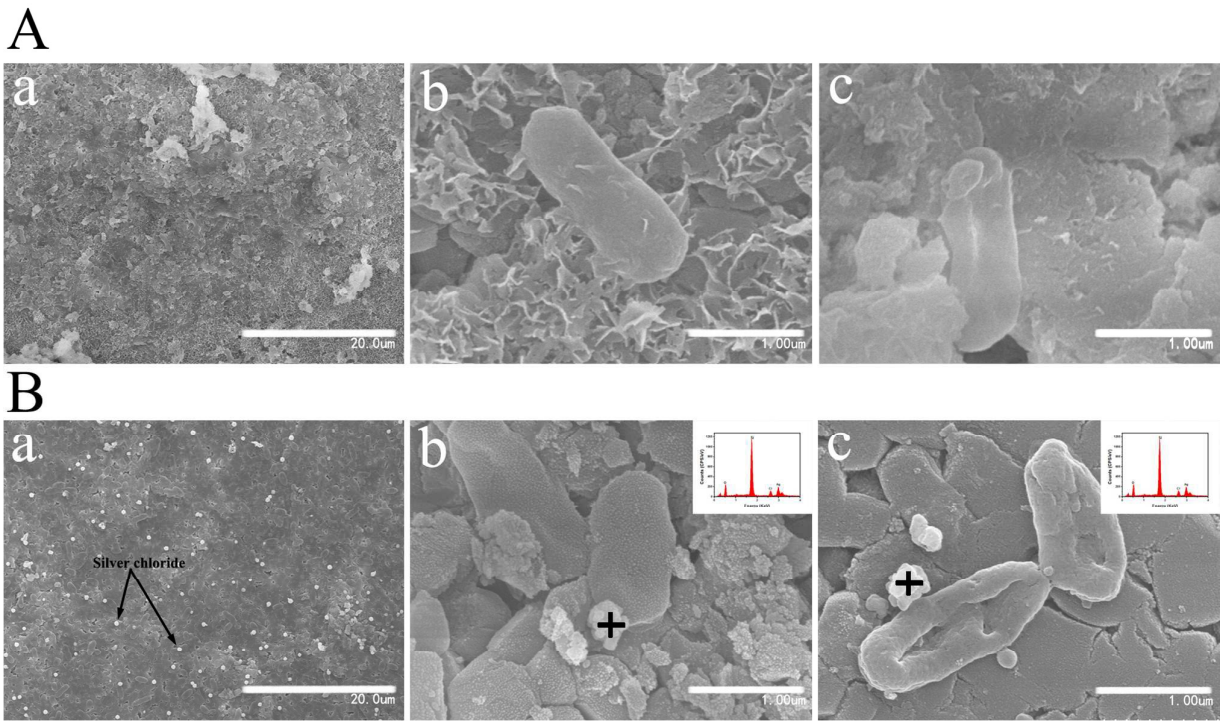

Fig 6. SEM morphology of E. coli seeded on CaMSS-0N-Ag and CaMSS-0.5N-Ag at different time. A, CaMSS-0N-Ag, a, low magnification at 30 min; b, c, high magnification at 30min and 60min, respectively. B, CaMSS-0.5N-Ag, a, low magnification at 30 min; b, c, high magnification at 30min and 60min, respectively; insert of b and c was the EDS characterize of the black crossing marked nanoparticles.

As we know that the typical morphology of E. coil is rod-shaped[20, 27]. After culturing for 30 min, the bacteria maintained its integrity and smooth edge without obvious damage on CaMSS-0N-Ag (Fig6A (b)) while shrank on CaMSS-0.5N-Ag (Fig 6B (b)). Nevertheless, after 60 min's treatment, cell shape distortion and wrinkle emerged on CaMSS-0N-Ag (Fig 6A (c)) and CaMSS-0.5N-Ag (Fig 6B (c)) plate surface and even serious membrane disruption existed on CaMSS-0.5N-Ag surface, leading to cytoplasm leakage and cell lysis.

The above results confirmed that the agglomerates of silver chloride were generated on the surface of CaMSS-0.5N-Ag, and the positively charged surface was beneficial to the E. coil adsorption. The generation of silver chloride indirectly proved that the silver ions were successfully tethered on the surface of amino functionalized CaMSS. These SEM images of CaMSS-0.5N-Ag (Fig 6B) revealedmore remarkable membrane dilapidation than CaMSS-0N-Ag (Fig 6A), whichwas also pointed outin the work of P. N. Lim *et al*[21]. Therefore, a conclusion could be drawn that it might be the silver chloride on the surface of CaMSS-0.5N-Ag that was responsible for antibacterial activity.

In vitro Cytotoxicity

As a potential material for clinical applications, cytotoxicity is of significant importance for CaMSS. MTT assays (Fig 7) conveyed that after co-culturing for 24 h for the cell viability at different concentrations of CaMSS, CaMSS-0N-Ag, CaMSS-0.5N-Ag and CaMSS-1N-Ag, there was no statistical difference ($p > 0.05$) between them. Compared with the negative control, the cell viability at all concentrations of CaMSS materials were slightly higher at 24 h, which may be related to the higher calcium leaching into the extracted fluid at an early period.

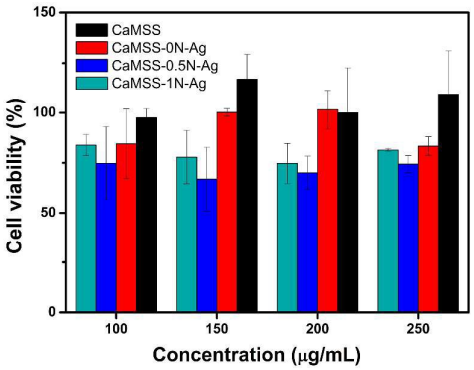

Fig7. Viability of myoblast cells after 24 h exposure to various materials and negative control. Data were obtained using MTT assay. Error bars represented means ± SD (n = 3).

This journal is © The Royal Society of Chemistry 20xx

RSC Advances Accepted Manuscript

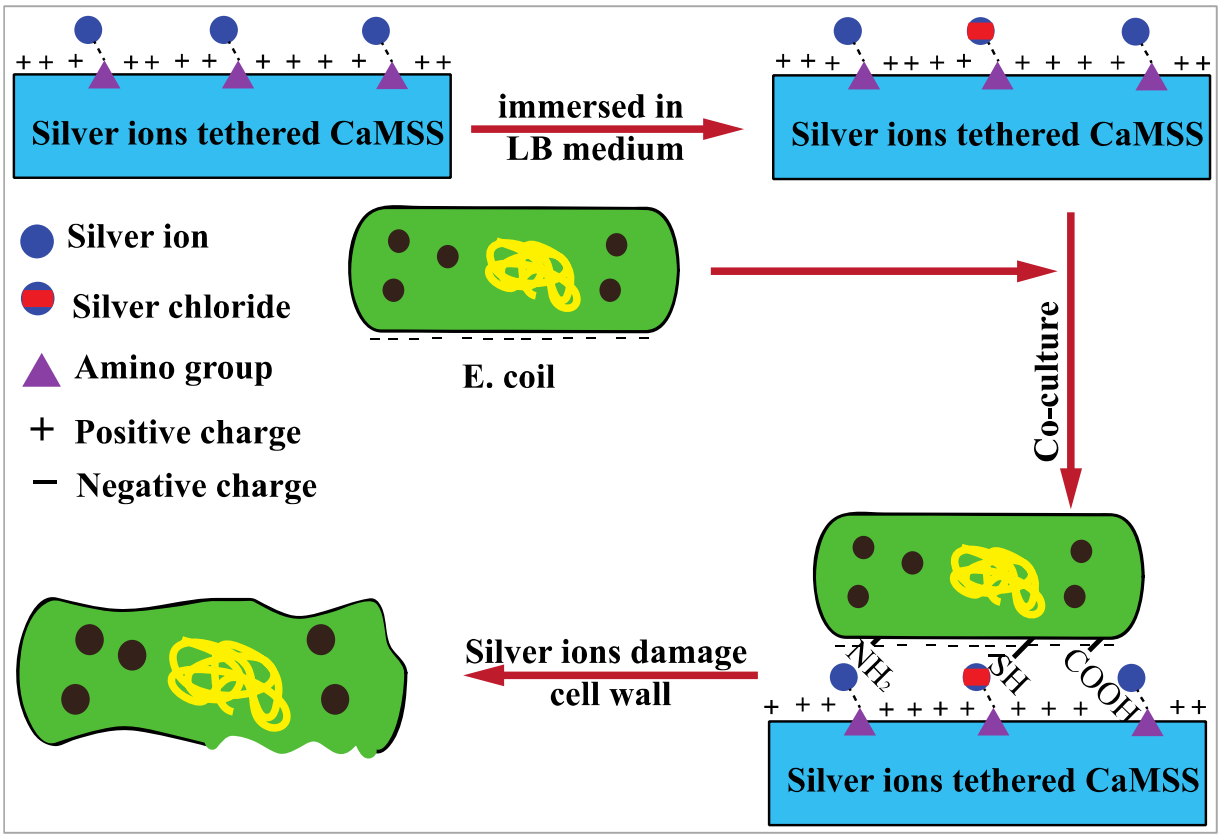

Fig 8. Schematic drawing of the proposed process of antibacterial action of silver loaded Amino-groups functionalized CaMSS.

However, the CaMSS-0N-Ag, CaMSS-0.5N-Ag and CaMSS-1N-Ag were more cytotoxic to C2C12 cell lines with all concentrations at 24 h.

The cytotoxicity results of CaMSS, CaMSS-0N-Ag, CaMSS-0.5N-Ag and CaMSS-1N-Ag indicated that the CaMSS had no cytoxicity to C2C12 cell in the test concentration and this result was well fitted into the results of antibacterial test. For CaMSS-0N-Ag, it exhibited a slight cytotoxicity compared with the CaMSS. However, CaMSS-0.5N-Ag and CaMSS-1N-Ag exhibited higher cytotoxicity than CaMSS and CaMSS-0N-Ag. We reckon, with the same Ag content, such cytotoxicity may arise from the amino-induced positive charge of CaMSS-0.5N-Ag and CaMSS-1N-Ag. In the future study, we are about to reduce the content of amino-group and lower the surface charge to endow CaMSS with excellent antibacterial activity and decreased cytotoxicity.

Above results suggested that CaMSS-0.5N-Ag and CaMSS-1N-Ag exhibited significant efficiency and more sustained inhibition on the growth of E. coli. Such variance in antibacterial ability might arise from the state of silver ion as well as different surface charge and functional group of CaMSS-0N-Ag, CaMSS-0.5N-Ag and CaMSS-1N-Ag [12]. For silver ions-absorbed CaMSS, silver ions were easy to release and fast to be consumedby the bacteria, giving rise to short-term antibacterial ability [28]. However, amino-based complexing action can offer a localized, concentrated and sustained silver ion, which made the surface-tethered silver ion or agglomerates of silver chloride available to directly deactivate biological groups by electrostatic interactions, inactivation of enzymes, and destruction of the cell wall, triggering the death of bacteria [17, 20-22], and maintain high antibacterial activity. Furthermore, the inversion of CaMSS surface charge from negative to positive may generate electrostatic interaction between the bacterial and amino-functionalized CaMSS, enhancing antibacterial ability. However, there's no obvious enhancement with the increase of positive charge. The comparable antibacterial activity of CaMSS-0.5N-Ag and CaMSS-1N-Ag indicated that the silver tethering played a more important role in the antibacterial activity than the surface positive charge.

Based on the above results and previous reports, the process of the antibacterial action of the silver ions tethered CaMSS hybrids was displayed in the following steps, as shown in Fig 8. Firstly, the chloride ions contained in the LB medium was absorbed to some of surface-tethered silver ions, forming

RSC Advances Accepted Manuscript

silver chloride agglomerates (confirmed by SEM and EDS, Fig 6B). Secondly, bacteria adhered onto the surface of CaMSS-0.5N-Ag, and silver ions or silver chloride agglomerates tethered onto the surface of CaMSS-0.5-Ag interacted with the cell envelope protein and enzymes of bacteria[17, 20-22], which may be strengthened by electrostatic interactions. Finally, the silver ions and silver chloride agglomerates triggered disruption of cell wall permeability, inactivation of enzymes, and thus led to death of the E. coil.

Conclusions

In the present study, silver ions were tethered onto calcium-doped meoporous silica for antibacterial applications. We also confirmed that the silver ions-tethered CaMSS hybrids exhibited enhanced and long-term antibacterial activity than the silver ions-adsorbed CaMSS. The comparable antibacterial activity of CaMSS-0.5N-Ag and CaMSS-1N-Ag indicated that the silver tethering had played a more important role in the antibacterial activity than the surface positive charge. From the clinical practical viewpoint, the silver ions tethered CaMSS hybrids may serve as a promising candidate in clinical treatment considering the rapid increase of resistances strains in clinical applications.

Acknowledgements

The authors wish to express their gratitude for financial support from the National Basic Research Program of China (973 Program, No. 2012CB933600), National Science and Technology Support Program (2014BAK05B02) and the 111 Project (B14018).

Notes and references

1. Y. Tian, H. Cao, Y. Qiao, F. Meng and X. Liu, *Acta biomaterialia*, 2014, **10**, 4505-4517.
2. C. T. Johnson and A. J. Garcia, *Annals of biomedical engineering*, 2015, **43**, 515-528.
3. J. Xue, M. He, Y. Niu, H. Liu, A. Crawford, P. Coates, D. Chen, R. Shi and L. Zhang, *International journal of pharmaceutics*, 2014, **475**, 566-577.
4. J. S. Lee and W. L. Murphy, *Adv Mater*, 2013, **25**, 1173-1179.
5.N. M. Mahmoodi, S. Khorramfar and F. Najafi, *Desalination*, 2011, **279**, 61-68.
6. M. Moritz and M. Geszke-Moritz, *Materials science & engineering. C, Materials for biological applications*, 2014, **41**, 42-51.
7. M. N. Sarvi, T. B. Bee, C. K. Gooi, B. W. Woonton, M. L. Gee and A. J. O'Connor, *Chemical Engineering Journal*, 2014, **235**, 244-251.
8. A. M. El-Toni, M. A. Habila, M. A. Ibrahim, J. P. Labis and Z. A. Alothman, *Chemical Engineering Journal*, 2014, **251**, 441-451.
9. Z. Chen, Z. Li, Y. Lin, M. Yin, J. Ren and X. Qu, *Biomaterials*, 2013, **34**, 1364-1371.
10. H. Zheng and S. Che, *RSC Advances*, 2012, **2**, 4421.
11. L. L. Li and H. Wang, *Advanced healthcare materials*, 2013, **2**, 1351-1360.
12. M. Liong, B. France, K. A. Bradley and J. I. Zink, *Advanced Materials*, 2009, **21**, 1684-+.
13. A. Braem, K. De Cremer, N. Delattin, K. De Brucker, B. Neirinck, K. Vandamme, J. A. Martens, J. Michiels, J. Vleugels, B. P. Cammue and K. Thevissen, *Colloids and surfaces. B, Biointerfaces*, 2015, **126**, 481-488.
14. N. Shadjou and M. Hasanzadeh, *Materials science & engineering. C, Materials for biological applications*, 2015, **55**, 401-409.
15. N. Ehlert, P. P. Mueller, M. Stieve, T. Lenarz and P. Behrens, *Chemical Society reviews*, 2013, **42**, 3847-3861.
16. C. Dai, Y. Yuan, C. Liu, J. Wei, H. Hong, X. Li and X. Pan, *Biomaterials*, 2009, **30**, 5364-5375.
17. J. Gehring, D. Schleheck, B. Trepka and S. Polarz, *ACS applied materials & interfaces*, 2015, **7**, 1021-1029.
18. Y. Tian, J. Qi, W. Zhang, Q. Cai and X. Jiang, *ACS applied materials & interfaces*, 2014, **6**, 12038-12045.
19. Y. Dong, T. Liu, S. Sun, X. Chang and N. Guo, *Ceramics International*, 2014, **40**, 5605-5609.
20. G. Jin, H. Qin, H. Cao, S. Qian, Y. Zhao, X. Peng, X. Zhang, X. Liu and P. K. Chu, *Biomaterials*, 2014, **35**, 7699-7713.
21. P. N. Lim, L. Chang, B. Y. Tay, V. Guneta, C. Choong, B. Ho and E. S. Thian, *ACS applied materials & interfaces*, 2014, **6**, 17082-17092.
22. Y. I. Seo, K. H. Hong, D. G. Kim and Y. D. Kim, *Colloids and surfaces. B, Biointerfaces*, 2010, **81**, 369-373.
23. C. Dai, C. Liu, J. Wei, H. Hong and Q. Zhao, *Biomaterials*, 2010, **31**, 7620-7630.
24. L. Pan, J. Liu, Q. He and J. Shi, *Adv Mater*, 2014, **26**, 6742-6748.
25. J. M. Rosenholm and M. Linden, *Chem Mater*, 2007, **19**, 5023-5034.
26. K. Waldron, W. D. Wu, Z. Wu, W. Liu, C. Selomulya, D. Zhao and X. D. Chen, *Journal of colloid and interface science*, 2014, **418**, 225-233.
27. J. Li, X. Liu, Y. Qiao, H. Zhu and C. Ding, *Colloids and surfaces. B, Biointerfaces*, 2014, **113**, 134-145.
28. A. Martinez-Abad, G. Sanchez, J. M. Lagaron and M. J. Ocio, *Food chemistry*, 2013, **139**, 281-288.

RSC Advances Accepted Manuscript

This journal is © The Royal Society of Chemistry 20xx

Tethering silver ion on Amino-functionalized mesoporous silica for enhanced and sustained antibacterial properties

Chengwei Wang,[a, b] Hua Hong,[a, c*] Zhaofen Lin,[c] Yuan Yuan, [a, c *], Changsheng Liu, [a, b, c*], Xiaoyu Ma,[a, b], Xiaoyan Cao,[a, b]

[a] Key Laboratory for Ultrafine Materials of Ministry of Education, East China University of Science and Technology, Shanghai 200237, PR China

[b] Engineering Research Center for Biomedical Materials of Ministry of Education, East China University of Science and Technology, Shanghai 200237, PR China.

[c] The Second Military Medical University, Shanghai 200433, PR China.

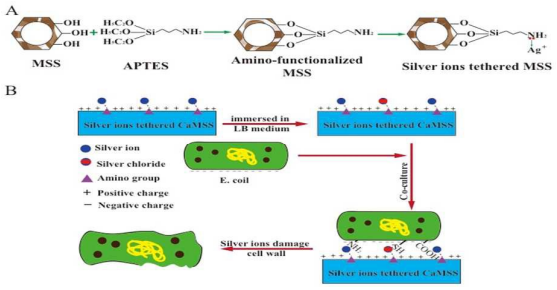

Amino group-based tethering method is an effective strategy to load Ag ion for long-term and high efficient antibacterial activity. And the developed Ag-CaMSS is a promising surgical implantation with excellent antibacterial activity.

RSC Advances Accepted Manuscript